Antinociceptive effects of the GPR55 antagonist CID16020046 injected into the rat anterior cingulate cortex

Bright N Okine[1, 3], Gemma Mc Laughlin[1], Jessica C Gaspar[1,3], Brendan Harhen[3], Michelle Roche[2, 3] and David P. Finn[1, 3*]

[1]Pharmacology and Therapeutics, [2]Physiology, School of Medicine, [3]Galway Neuroscience Centre and Centre for Pain Research, NCBES, National University of Ireland, Galway, University Road, Galway, Ireland

*Corresponding author: Professor David Finn (david.finn@nuigalway.ie), Pharmacology and Therapeutics, National University of Ireland Galway, University Road, Galway, Ireland. Tel: +353 (0)91 495280, Fax: +353 (0)91 495586

Running title: *GPR55 and pain*

Category: Original article

Number of pages: 35

Number of Figures: 5

Disclosures: The authors have no conflicts of interest to declare.

List of abbreviations

2-AGPI- 2-arachidonoyl-sn-glycero-3-phosphoinositol

ACC- Anterior cingulate cortex

BSA- Bovine serum albumin

DMSO- dimethylsuphoxide

ERK- extracellular signal- regulated kinase

GFAP- Glial fibrillary acidic protein

GPR55- G- protein couple receptor 55

Iba-1-ionized calcium-binding adapter molecule 1

LC-MS/MS- Liquid chromatography tandem mass spectrometry

LPI- lysophosphatidylinositol

MAPK- mitogen activate protein kinase

NeuN- Hexaribonucleotide Binding Protein-3

PAG-periaqueductal grey

PBST- Phosphate buffered saline-Tween

PFA- paraformaldehyde

qRT-PCR- quantitative real time polymerase chain reaction

RIPA- radio immunoprecipitation assay

SD- Sprague-Dawley

SDS-PAGE- sodium dodecyl sulphate polyacrylamide gel electrophoresis

TBST- Tris buffered saline - Tween

Abstract

The G-protein coupled receptor, GPR55, modulates nociceptive processing. Given the expression of GPR55 in the anterior cingulate cortex (ACC), a key brain region involved in the cognitive and affective dimensions of pain, the present study tested the hypothesis that GPR55 signalling in the ACC facilitates inflammatory pain behaviour in rats. The expression of GPR55 in the ACC was confirmed by both western blotting and immunostaining, with evidence for neuronal localisation. Microinjection of the selective GPR55 antagonist CID16020046 into the ACC of adult male Sprague-Dawley rats significantly reduced second phase formalin-evoked nociceptive behaviour compared with vehicle-treated controls. CID16020046 administration was associated with a reduction in phosphorylation of extracellular signal-regulated kinase (ERK), a downstream target of GPR55 activation, in the ACC. Intra-ACC administration of CID16020046 prevented the formalin-induced increases in expression of mRNA coding for the immediate early gene and marker of neuronal activity, *c-Fos*, in the ipsilateral dorsal horn of the spinal cord. Intra-plantar injection of formalin reduced tissue levels of the endogenous GPR55 ligand 2-arachidonoyl-sn-glycero-3-phosphoinositol (2-AGPI) in the ACC, likely reflecting its increased release/utilisation. These data suggest that endogenous activation of GPR55 signalling and increased ERK phosphorylation in the ACC facilitates inflammatory pain via top-down modulation of descending pain control.

Keywords: c-Fos; CID16020046; ERK; GPR55; Pain; Prefrontal cortex

The G-protein coupled receptor, GPR55, is now recognised as an endogenous receptor target for bioactive phospholipids and endocannabinoids (Ross, 2009, Sharir and Abood, 2010). GPR55 activation is linked with the modulation of multiple intracellular signalling pathways, in particular the activation of extracellular signal-regulated kinases 1 and 2 (ERK1/2) within the mitogen-activated protein kinase (MAPK) signalling cascade. Recent studies have also implicated GPR55 in an array of physiological and pathophysiological processes, including a modulatory role in nociceptive processing (Breen et al., 2012, Gangadharan et al., 2013, Guy et al., 2015, Schuelert and McDougall, 2011, Staton et al., 2008, but see also Carey et al., 2017).

However, the neuroanatomical sites within which GPR55 modulates nociceptive processing remain poorly understood. One recent study showed that injection of L-α-lysophatidylinositol (LPI), an endogenous agonist of GPR55 (Oka et al., 2007), into the midbrain periaqueductal grey (PAG), was associated with a reduction in nociceptive threshold or increased sensitization to an acute thermal noxious stimulus in rats (Deliu et al., 2015). The PAG is a key component of the descending pain pathway, an endogenous pain modulatory system, the activation of which alters nociceptive transmission at the level of the spinal cord dorsal horn (Ossipov et al., 2010, Basbaum and Fields, 1984). The components of the descending pain pathway, in particular the PAG, are also subject to modulation by other higher brain centres, in particular the anterior cingulate cortex (ACC) (Fuchs et al., 2014, Shackman et al., 2011, An et al., 1998, Valet et al., 2004). The ACC plays a key role in the modulation of cognitive and affective components of pain (Barthas et al., 2015, Donahue et al., 2001, Fuchs et al., 2014, Johansen et al., 2001, Qu et al., 2011, Rainville et al., 1997).

The expression of GPR55 in the ACC has previously been reported (Henstridge et al., 2011), however, the functional relevance or contribution of GPR55 signalling in the ACC to pain processing is unknown. In view of the anatomical connectivity between the ACC and the

descending pain pathway, and the recent evidence of a key role for GPR55 signalling in the PAG in nociceptive processing, the present study investigated whether GPR55 signalling in the ACC contributes to nociceptive responding in an animal model of inflammatory pain.

Thus, working with the hypothesis that selective blockade of GPR55 in the ACC will reduce inflammatory pain-related behaviour, we investigated the effects of the selective GPR55 antagonist, CID16020046 (Kargl et al., 2013), on formalin-evoked nociceptive behaviour in rats. In order to identify possible molecular mechanisms underlying the effects of CID16020046, we measured ERK protein phosphorylation, a downstream target of GPR55 activation, in the ACC. The effects of CID16020046 injection into the ACC on the activity of the descending pain pathway were determined by measuring expression of c-*Fos* in the spinal cord dorsal horn, a molecular correlate of descending pain pathway activity. Evidence from mass spectrometric analysis and activity binding assays suggest that endogenous LPI in the rodent brain is comprised of a variety of molecular species which differ in their fatty acid moieties. The arachidonic acid containing species, 2-arachidonoyl-sn-glycerol-3-phosphoinositol (2-AGPI) is considered to be the most potent species at GPR55 (Oka et al., 2009). Thus, in a separate group of rats, the effect of intra-plantar formalin injection on 2-AGPI levels in the ACC was determined using liquid chromatography-tandem mass spectrometry (LC-MS/MS). Expression of GPR55 in the ACC was also investigated using western blotting and immunofluorescence histochemistry.

Materials and Methods

Animals

Adult male Sprague-Dawley rats (n=22, Experiment 1) weighing 225-250g, were obtained from Harlan (Bicester, UK). Animals were housed in groups of three to four prior to surgery and singly housed post-surgery in plastic bottomed cages (45x20x20 cm) containing wood

shavings as bedding. Animal housing rooms were maintained at a constant temperature (21°C ± 0.5°C) under standard lighting conditions (12:12 h light : dark, lights on from 07:00 to 19:00 h). Food and water were provided ad libitum. Adult male Sprague-Dawley rats used in Experiment 2 (n=11, 225-250g) were bred in-house and housed under similar conditions and time lines to rats in Experiment 1 without undergoing any surgical procedures. All *in vivo* procedures were approved by the Animal Care and Research Ethics Committee, National University of Ireland, Galway, and carried out under license from the Irish government in accordance with EU Directive 2010/63/EU and ARRIVE guidelines (Kilkenny et al., 2010).

Intra-ACC guide cannulae implantation

Implantation of guide cannulae into the ACC was carried out as previously described (Okine et al., 2014). In brief, rats were implanted stereotaxically with stainless steel guide cannulae (5mm length, 0.71 mm outer diameter, Plastics One Inc, Roanoke, VA, USA), bilaterally 1mm above the target injection site within the ACC (anteroposterior + 1.5mm, mediolateral ± 1.3mm relative to bregma at an angle of 12°, dorsoventral – 1.3 mm from dura) (Figure 1A), under isoflurane anaesthesia (1-3% in O_2 ; 0.60 L/min). The cannulae were permanently fixed to the skull using stainless-steel screws and carboxylate cement. A stainless steel stylet (Plastics One Inc) was inserted into each guide cannula to prevent blockage by debris. The non-steroidal anti-inflammatory agent carprofen (5mg/kg subcutaneously; Rimadyl, Pfizer, Kent, UK), was administered during surgery to manage postoperative pain. The antibiotic enrofloxacin (2.5mg/kg subcutaneously; Baytril, Bayer Ltd., Dublin, Ireland) was administered on the day of surgery and for 4 consecutive days after surgery to prevent infection. Rats were allowed a period of 7-8 days to recover from surgery before formalin testing. Body weight and general health were monitored daily during the recovery period.

Chemicals and drug preparation

The GPR55 antagonist, CID16020046 (cat# SML0805, Sigma-Aldrich, Dublin, Ireland), was administered in 100% dimethylsulfoxide (DMSO) vehicle at a concentration of 10µM. This concentration of CID16020046 was chosen on the basis of *in vitro* studies demonstrating the ability of the drug to block the effects of LPI-mediated activation of GPR55 in mammalian cell lines (Kargl et al., 2013) and the relative absence of mixed agonist/antagonist effects associated with other well characterised antagonists of GPR55 notably ML193 and cannabidiol (Heynen-Genel S, 2010, Viudez-Martínez et al., 2017). 100% DMSO has been used widely in previously published pain-related intracerebral microinjection studies from our group and other groups (Finn *et al.*, 2003; Hohmann *et al.*, 2005; Suplita *et al.*, 2005; Connell *et al.*, 2006; Roche *et al.*, 2007; Roche *et al.*, 2010; Olango *et al.*, 2011; Okine *et al.*, 2014; Rea *et al.*, 2014). Moreover, in order to determine whether intra-ACC administration of 100% DMSO has effects on formalin-evoked nociceptive behaviour, we collated data from previous studies carried out in our laboratory and performed a statistical analysis of composite pain scores between naïve rats and rats that received intra-ACC administration of 100% DMSO for the first 30 minutes post-formalin, the period during which the majority of pharmacological effects were observed in our studies (Naive: 0.61 ±0.39 and DMSO 0.67 ± 0.29, Mean ± SEM composite pain score data). Repeated measures ANOVA did not reveal any significant differences between the two groups of rats, indicating that intra-ACC administration of 100% DMSO has no effect on formalin-evoked nociceptive behaviour thus ruling out any confounding effects on the effects of CID16020046. Formalin (2.5%) was prepared from a 37% stock solution of formaldehyde (cat# F1635, Sigma-Aldrich, Dublin, Ireland) diluted in 0.9% sterile saline.

Experimental procedures

Rats were randomly assigned to treatment groups. The sequence of testing was also randomized equitably across the experimental days to minimise its potential influence as a source of variability. CID16020046 (10µM) or vehicle was microinjected (outer diameter of injection needle 0.36mm) into the ACC in a volume of 0.5 µL per side over 60 seconds (with injectors left in place for an additional 60 seconds to allow diffusion of drug away from the injector tip) using an injector and Hamilton syringe attached to polyethylene tubing. Immediately thereafter, rats were placed in a perspex chamber (30x30x40 cm, 30 lux) with blackened walls for the assessment of horizontal locomotor activity as well as rearing and grooming behaviours for 10 minutes. A video camera located beneath the chamber was used to record animal behaviour for subsequent analysis. Immediately after this 10 minute pre-formalin trial, rats received an intra-plantar injection of 50 µL formalin (2.5% in 0.9% sterile saline) into the right hind-paw under brief isoflurane anaesthesia as described previously (Finn et al., 2003, Roche et al., 2007). Following formalin injection, rats were immediately returned to the perspex chamber for a period of 60 minutes. Formalin-induced oedema was measured as the change in diameter of the right hindpaw measured immediately before formalin administration and at the end of the experiment using Vernier callipers. Behaviours during the formalin trial were rated as described previously (Okine et al., 2014, Rea et al., 2014, Finn et al., 2003, Roche et al., 2007). Briefly, EthoVision XT software package (Noldus Information Technology, Wageningen, The Netherlands) was used to analyze behaviour. Ethovision allowed for continuous event recording over the 10-minute pre-formalin and 60-minute post-formalin trials for each rat. A trained observer, blind to the experimental conditions, assessed behaviour. Formalin-evoked nociceptive behaviour was scored according to the weighted composite pain scoring technique described by (Watson et al., 1997). This method categorized pain behaviours as time spent raising the injured hind paw above the floor without contact with any other surface (Pain 1) and biting, licking,

holding, flinching or shaking the paw (Pain 2). These values were used to calculate the composite pain score: CPS = (Pain 1 + 2[Pain 2])/total duration of analysis period). At the end of the 60-minute formalin trial, rats were killed by decapitation, brain and spinal cord tissues harvested and snap-frozen for post-mortem analysis of ERK protein phosphorylation in the ACC and *c-Fos* mRNA in the spinal cord dorsal horn.

Histological verification of intra-cerebral microinjection sites

Intra-cerebral microinjection sites were verified by bilateral injections of fast-green dye (1% in DMSO) into the ACC post-mortem. Representative cryosections of the ACC (30µm thickness) were collected and mounted on gelatinised glass slides and viewed under light microscope for precise verification of cannula / injector placement in the ACC. Only rats with correctly placed microinjections (~70% of total number of rats in the experiment, Figure 1A) were included in final analysis of behavioural data. The remainder of the ACC was cryosectioned and punched for measurement of ERK protein phosphorylation. Frozen coronal brain sections (150µm thickness) at the level of the ACC (AP +1.5 to -1.0mm), based on rat brain atlas of (Paxinos and Watson, 1986), were cut on a cryostat (MICROM GMBH, Stuttgart, Germany). The ACC was then punch-dissected from sections using 2mm cylindrical brain punchers (Harvard Apparatus, Holliston, MA, USA) as described previously (Okine et al., 2014). The mean ± standard error of mean (SEM) weight per rat of the punch-dissected ACC tissue was 10 ± 2.0 mg.

Western blotting

Western blotting was performed as described previously (Okine et al., 2012a) with minor modifications. Briefly, frozen punches of ACC tissue weighing approximately 10 mg were lysed by brief sonication in RIPA lysis buffer, (1:10 w/v), in a 1.5ml microcentrifuge tube. The homogenate was placed on a shaker for 45 minutes at 4°C with gentle agitation to allow for complete dissociation of nucleo-protein complexes, followed by centrifugation at 16000g (Eppendorf Centrifuge 5415R, Stevenage, UK) for 20 minutes at 4°C. The supernatant was collected and protein content determined by Bradford assay (Bradford, 1976). Thirty micrograms of protein sample in 4X Laemmli sample loading buffer was boiled at 100°C for 5 minutes, briefly centrifuged and subjected to 9% sodium dodecyl sulphate polyacrylamide gel electrophoresis (SDS-PAGE) at a constant voltage of 120V for 2 hours. The separated protein samples were electro-blotted onto a nitrocellulose membrane (Nitrocellulose membrane, CAS# 9004-70-0, Bio-Rad, Dublin, Ireland) at 100V for 1 hour. Protein transfer efficiency was verified by Ponceau dye (0.1% dye in 5% acetic acid) staining. Membranes were blocked in 5% non-fat dry milk in 0.1% Tris-buffered saline / Tween20 (TBST) solution for 1hr at room temperature and incubated overnight at 4^{o}C with rabbit polyclonal antibody to GPR55 (cat# orb101191, Biorbyt, UK), total ERK1/2 (cat# 9102, Cell Signalling, UK,) or phospho-ERK1/2 (cat# 9101, Cell Signalling, UK,) diluted 1,200, 1:1000 and1:1000 respectively in 5% milk/0.1% TBST. The detection of both total and phosphorylated ERK1/2 immunoreactive bands were simultaneously performed on two replica gels containing identical amount of protein and loading order for each sample, and subjected to identical electrophoretic conditions. Membranes were subjected to 3 x 10 minute washes in 0.1% TBST and incubated with secondary antibody solution containing IRDye® conjugated goat anti-rabbit (λ800) (LI-COR® Biosciences Abingdon Park, Oxford UK) diluted 1:10000 in 1% milk/ 0.1% TBST for one hour at room temperature. Three x 5 minute washing steps were then performed with washing solution and one final 5 minute wash in distilled H_2O. Blots were scanned on a LI-

COR® Odyssey imager. IR band intensities for total and phosphorylated ERK(1/2) protein expression (~ 44kDa for ERK 1 and ~ 42kDa for ERK 2) for each sample were generated automatically using the background subtraction method of the LI-COR Image Studio® Ver. 2.0 imaging software. The ratio of phosphorylated ERK(1/2) band intensity to total ERK (1/2) band intensity was then calculated for each sample, and then expressed as a % of mean vehicle-treated group values.

GPR55 immunofluorescence histochemistry in the ACC

One rat was used for the qualitative immunoflourescence analysis of the expression of GPR55 in the ACC. The rat was trans-cardially perfused under pentobarbital (60mg/kg) anaesthesia with heparanised 0.9% saline solution followed by 4% paraformaldehyde (PFA) as fixative. The brain was harvested and post-fixed for 24hrs in 4% PFA solution followed by cryoprotection in 25% sucrose-azide solution and cut on a cryostat (Bright instruments, UK) at a thickness of 20µm. Sections containing the ACC based on the coordinates obtained from rat brain atlas were collected and fixed to superfrost plus slides (VWR, UK). An antigen retrieval step was performed prior to immunostaining to enhance antibody-antigen interaction. Briefly, slides were immersed in citrate buffer solution, pH6 and boiled in a microwave for 10 minutes, followed by brief rinsing in distilled water and simmering for a further 10 minutes in the microwave. Immunofluorescence histochemistry was performed according to standard procedures. Briefly slides were washed in a solution of phosphate buffered saline 0.1% Tween20 (PBST), blocked in 3% BSA for 1hr and incubated overnight with rabbit polyclonal primary antibody raised against GPR55 (1:200, cat# orb101191, Biobyrt UK) alone, or separately in combination with mouse monoclonal primary antibodies raised against the neuronal marker NeuN (1:300, cat# ab104224, abcam UK) or astrocyte marker GFAP (1:300, cat# 3898, sigma, UK) or goat polyconal antibody raised against the marker for microglia,

IBA1 (1:100 cat# ab 104159, abcam, UK) overnight at room temperature. Slides were washed in PBST solution and further incubated in a solution containing secondary antibodies raised in goat or donkey against rabbit or mouse (1:500, Alexa fluor, thermofisher, UK) as appropriate at room temperature for 2hrs. Sections were washed and mounted in Vectashield mounting medium (cat# 101098-042, Vector laboratories, USA) and cover-slipped for qualitative microscopic analysis. A no primary antibody (anti-GPR55) condition was included as negative control for GPR55. Images were captured on a Zen Confocal microscope at X10 magnification.

Quantitative real time polymerase chain reaction (qRT-PCR)

Total RNA was extracted from post-mortem ipsi and contralateral spinal cord tissues and processed for cDNA synthesis as previously described (Okine et al., 2012b). Taqman gene expression assay for rat *c-Fos* (assay ID - Rn 02396759_m1, Applied Biosystems, UK) containing forward and reverse primers and a FAM-labelled MGB Taqman probe was used to quantify genes coding for *c-Fos* mRNA on a '*StepOne Plus'* instrument (Applied Biosystems, Warrington, UK). VIC-labelled *GAPDH* (assay ID 4308313 Applied Biosystems, Warrington, UK) was used as the housekeeping gene and endogenous control. A no template control reaction was included in all assays. The relative expression of target genes to endogenous control was calculated using the formula $2^{-\Delta Ct}$, where ΔCt represents the magnitude of the difference between cycle threshold (Ct) values of the target and endogenous control, and the result expressed as a percentage of the mean value of the contralateral vehicle group.

Quantitation of the endogenous GPR55 ligand, 2-arachidonoyl-sn-glycerol-3-phosphoinositol (2-AGPI) in ACC tissue using liquid chromatography—tandem mass spectrometry (LC-MS/MS)

The levels of 2-AGPI, a potent endogenous agonist of GPR55, were measured in the ACC of separate groups of rats, 30 mins after they had received intraplantar injections of formalin or saline into the right hind-paw. The method of 2-AGPI extraction from post-mortem tissues was adapted from previously published methods (Masquelier and Muccioli, 2016, Oka et al., 2009). Briefly, microdissected frozen ACC punches ~ 5mg were homogenised by sonication in 200µL of a medium containing Chloroform: Methanol: 2M HCl (2:1:1 v/v) spiked with 50ng (or 26.6µL of 1.875ng/µL stock solution) of 1-(10Z-heptadecenoyl)-sn-glycero-3-phospho-1'-myo-inositol) (cat# 110718, Avanti lipids, USA) included as internal standard. The homogenate was centrifuged at 10000 rpm for 10 minutes at 4^{o}C and the chloroform (organic) layer containing 2-AGPI was collected for analysis by LC-MS/MS. Mobile phase Solvent A was millipore grade water containing 0.1% v/v Formic acid and solvent B was LC/MS grade acetonitrile containing 0.1% v/v formic acid. Samples were separated on a ACE3 C18 PFP column (dimensions 100mm length, 2.1mm internal diameter, 3µm particles, Cat# ACE-1110-1002, ACE, UK) by reversed-phase gradient elution. Gradient programme was 10% solvent B for one minute, then ramped linearly up to 100% solvent B over 9mins and held at this for a further 10 mins.. Analyte detection was carried out in electrospray-negative ionization and multiple reaction monitoring (MRM) mode on an Agilent 1100 HPLC system coupled to a triple quadrupole 6460 mass spectrometer (Agilent Technologies Ltd, Cork, Ireland). MRM transitions were 619.3 to 303.3 for 2-AGPI and 583.3 to 241.2 for the internal standard, with fragmentor voltage at 130V and collision energy at 40eV. Under these conditions, 2-AGPI eluted at a retention time of 10.5 mins . Quantification of 2-AGPI was performed by ratiometric

analysis of peak areas of 2AGPI: internal standard and extrapolation on a 10-point calibration curve (0.072ng-18.75µg) derived from a four-fold dilution of a synthetic 2-AGPI analogue, 1-arachidonoyl-2-hydroxy-sn-glycerol-3-phosphoinositol (cat # 80105P, Avanti lipids, USA). The concentration of 2-AGPI was expressed in nmol g^{-1} of tissue. The limit of quantitation was 29ng on column.

Data analysis

SPSS statistical software (SAS Institute Inc, Ireland) was used to analyse all data. Parametric statistical tests were performed if the dataset passed the Kolmogorov-Smirnov's (KS) normality test, and if the F-test for comparison of variances did not reveal any significant differences in between datasets. Where only one of these conditions was met, a Student's t-test with Welch's correction was used for pairwise group comparisons. Locomotor activity (distance moved), general rat behaviours (rearing and grooming) during the preformalin trial were analysed by Student's unpaired, two-tailed t-test. Formalin-evoked nociceptive behaviour (CPS, Pain 1 and Pain 2) data were analysed by one-way repeated measures ANOVA with treatment and time considered as between-subject and within-subject factors, respectively. Student's unpaired, two-tailed t-test was used for comparison of specific time points between the two groups where appropriate. ERK protein data, c-*Fos* mRNA data were analysed by Student's unpaired, two-tailed t-test. LC-MS/MS data were analysed with Student's unpaired, two-tailed t-test with Welch's correction due to a significant difference in variances, although the KS normality test was passed. Data were considered significant when $p<0.05$. Results are

expressed as group means ± SEM. Individual data points are superimposed on bar graphs to show distribution of data.

Results:

GPR55 protein is predominantly expressed on neurons in the ACC

The qualitative expression of GPR55 in the ACC was confirmed by both western blotting (WB) and immunostaining techniques. Analysis by WB revealed immunoreactive bands corresponding to the predicted molecular weight of GPR55 of approximately 37kDa (Figure 1B). A non-specific band, possibly unidentified splice variant of GPR55 of approximately 30 kDa was also observed. A whole rat brain lysate was included in the analysis as a positive control. Further qualitative analysis by immunofluorescence also revealed positive immunostaining for GPR55 in the ACC (Figure 1C) which was strongly co-localised with the neuronal marker NeuN, but not GFAP (astrocyte marker) or the marker for microglia, IBA-1 (Figure 1C).

Fig 1

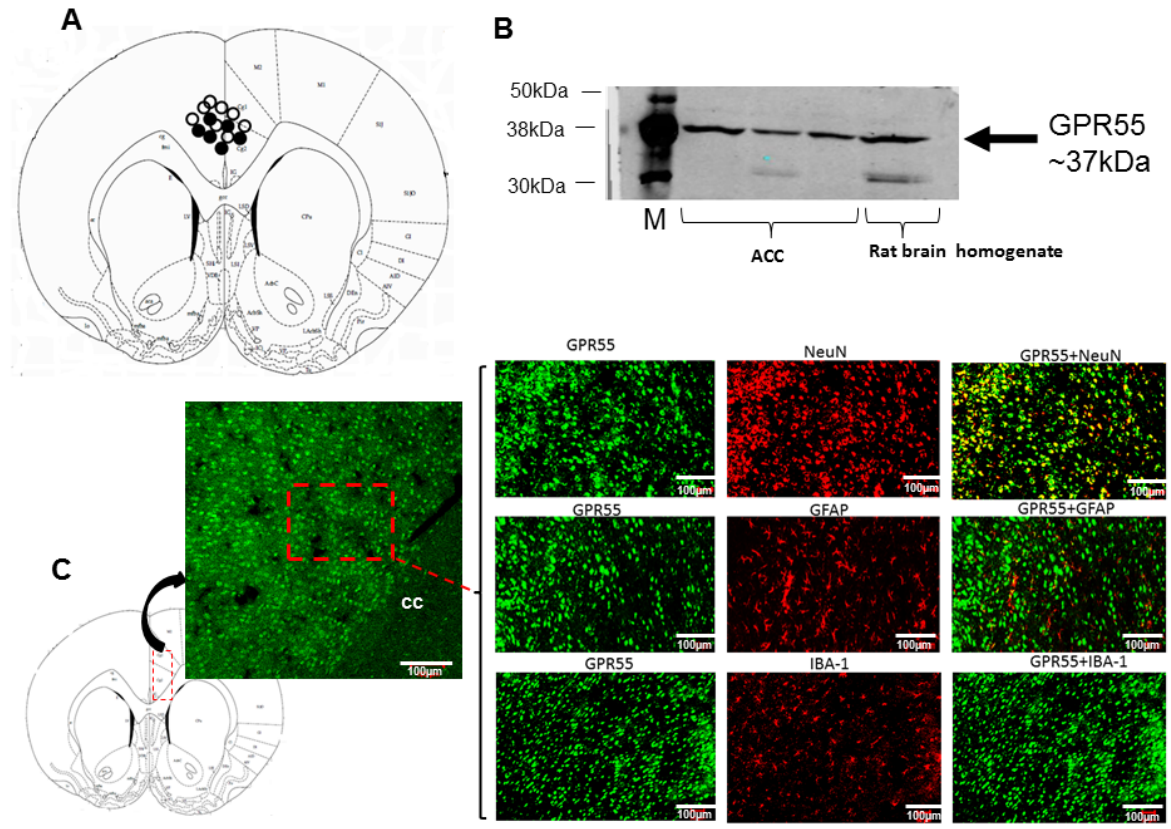

Figure 1. (A) Schematic depicting microinjection sites in the rat ACC. Image was taken from the rat brain atlas of Paxinos and Watson (2006) AP=~ +1.6mm. open circles = Vehicle, closed circles=CID16020046. n =6-8 rats per group **(B) Expression of GPR55 protein in the rat ACC**. Western blotting analysis of GPR55 expression revealed strong immunoreactive bands of approximately 37kDa in the ACC and whole rat brain homogenates (positive control). M: molecular weight marker **(C) Qualitative immunostaining for GPR55, NeuN, GFAP and IBA-1 in the ACC**. GPR55 images from n=3 separate sections taken at X10 magnification. NeuN- neuronal marker, GFAP- astrocyte marker, IBA-1, marker for microglia, cc-corpus callosum.

Intra-ACC administration of CID16020046 does not alter preformalin locomotor activity, rearing or grooming

Intra-ACC administration of CID16020046 did not alter preformalin locomotor activity (distance moved in arena) in rats compared with vehicle-treated counterparts [Veh vs CID: 1374±74.95cm, n=8 vs 1279±125.4cm, n=6] or the duration of rearing [Veh vs CID: 79±11.01s, n=8 vs. 106.1±16.77s, n=6] and grooming [Veh vs CID: 44.7±11.15s, n=8 vs 54.73± 22.27s, n=6] behaviours ; data are mean±SEM, unpaired Student's t-test $p>0.05$).

Fig 2

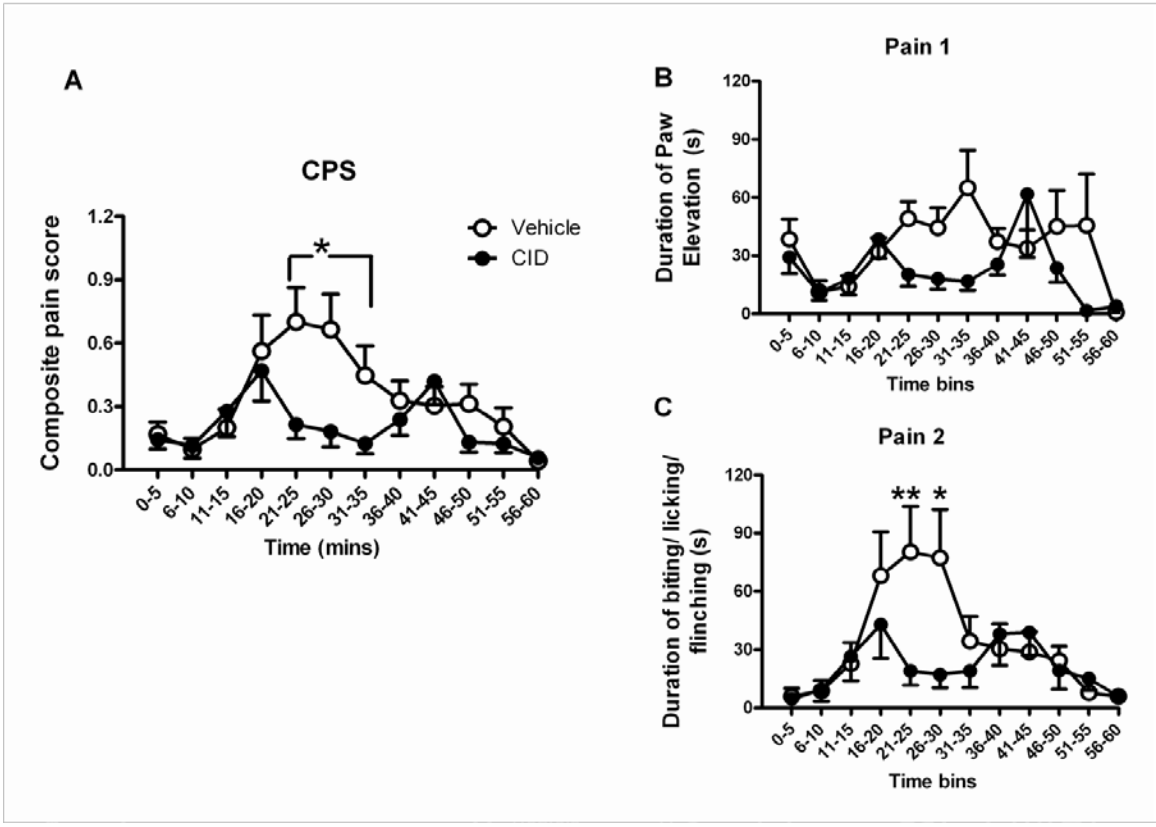

Figure 2. Effects of bilateral microinjections of CID16020046 into the ACC on formalin-evoked nociceptive behaviour in rats. Intra-ACC administration of the selective GPR55 antagonist, CID16020046, significantly reduced (A) the composite pain score during the

second phase from 21-35mins post-formalin, and (C) duration of licking/biting/flinching behaviour (Pain 2) from 21-30 mins post-formalin, compared with vehicle-treated counterparts, with no significant effect on (B) duration of paw elevation. Data are means ± SEM. *p<0.05 and**p<0.01, CID16020046 vs Vehicle. Repeated measures ANOVA followed by Student's unpaired t-test. Vehicle n = 8, CID16020046, n = 6 rats per group. Pain 1: duration of paw elevation, Pain 2: duration of licking/ biting/flinching.

Intra-ACC administration of CID16020046 reduces formalin-evoked nociceptive behaviour

Analysis of formalin-evoked nociceptive behaviour (as composite pain score) by repeated measures ANOVA revealed significant main effects of treatment ($F_{(11,132)}$=4.95, p=0.046), time ($F_{(11,132)}$=4.19, p<0.0001) and treatment x time interaction ($F_{(1,12)}$=2.06, p=0.028). Further temporal analysis by unpaired Student's t-test revealed a significant (p<0.05) reduction in the peak of second phase (t=21 to t=35 mins) of formalin-evoked nociceptive behaviour in rats that received CID16020046 microinjections into the ACC, compared with vehicle-treated counterparts (Figure 2A). Further analysis of the component pain-related behaviours revealed that CID16020046 significantly reduced the duration of biting/licking/flinching behaviour (Pain 2) during the second phase of the formalin trial (Figure 2C). Duration of paw elevation (Pain 1) during the second phase was also lower in CID16020046-treated rats but this effect did not reach statistical significance (Figure 2B).

Intra-ACC administration of CID16020046 had no significant effect on formalin-induced hind paw oedema (Veh: 1.95 ±0.49mm, n=8 versus CID16020046: 1.69 ± 0.17mm, n=6, Mean ± SEM).

Intra-ACC administration of CID16020046 reduced formalin-evoked ERK phosphorylation in the ACC

Injection of CID16020046 into the ACC tended to reduce (p=0.06) total ERK1/2 protein phosphorylation in the ACC (Figure 3Ai & ii), compared with vehicle-treated counterparts. This effect was significant (p<0.05) for the ERK1 isoform alone (Figure 3B), with a similar albeit non-significant (p>0.05) trend in the same direction for the ERK2 isoform (Figure 3C).

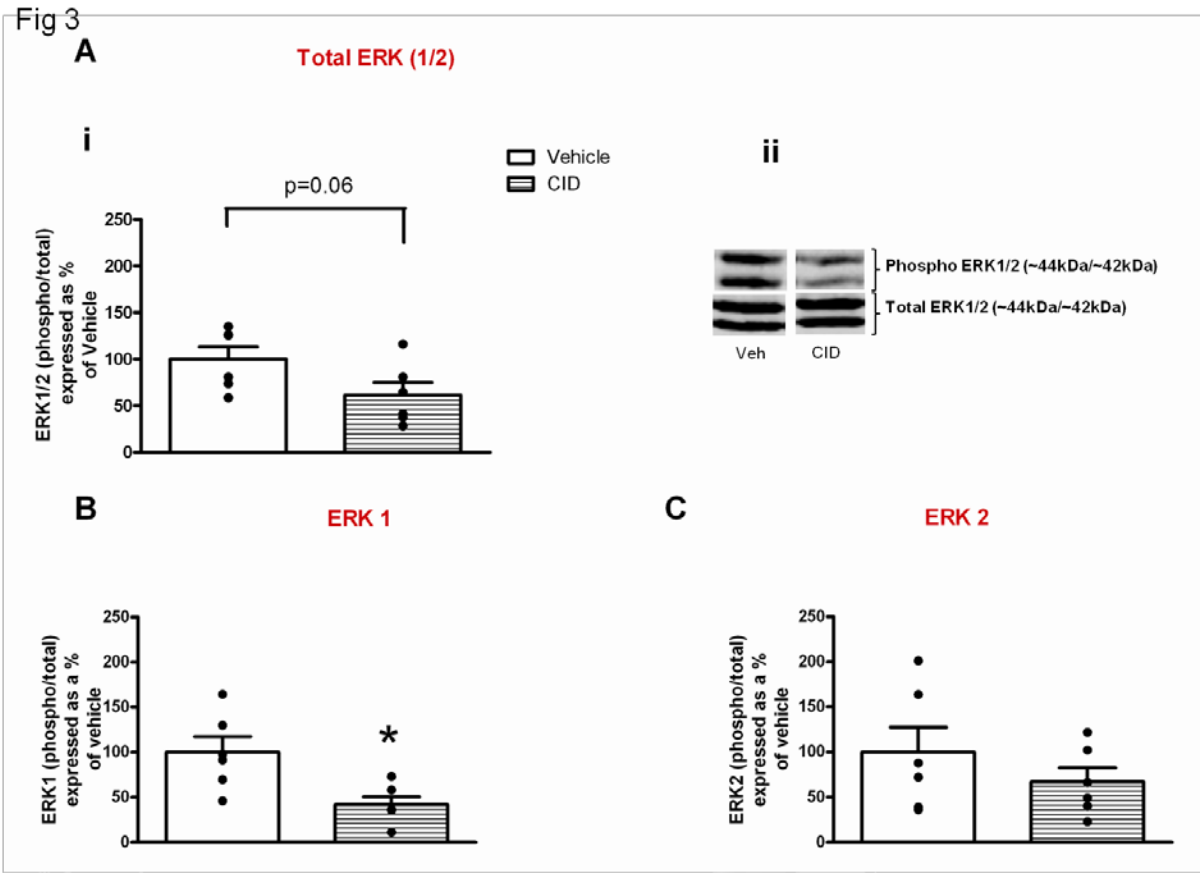

Figure 3. Western blotting analysis of ERK (1/2) protein phosphorylation in the ACC. (Ai & Aii) Intra-ACC administration of CID16020046 robustly reduced total ERK phosphorylation in the ACC compared with vehicle-treated rats. **(B & C)** Effects of CID16020046 on phosphorylation of ERK 1 and 2 isoforms, respectively. Data are means ± SEM. * p<0.05, CID16020046 vs Vehicle. Individual data points superimposed as black dots

on bar graphs. Student's unpaired t-test. Vehicle n = 8 and CID16020046, n = 6 rats per group. ERK: extracellular signal-regulated kinase, ACC: anterior cingulate cortex. Data are mean ± SEM, *p<0.05

Fig 4

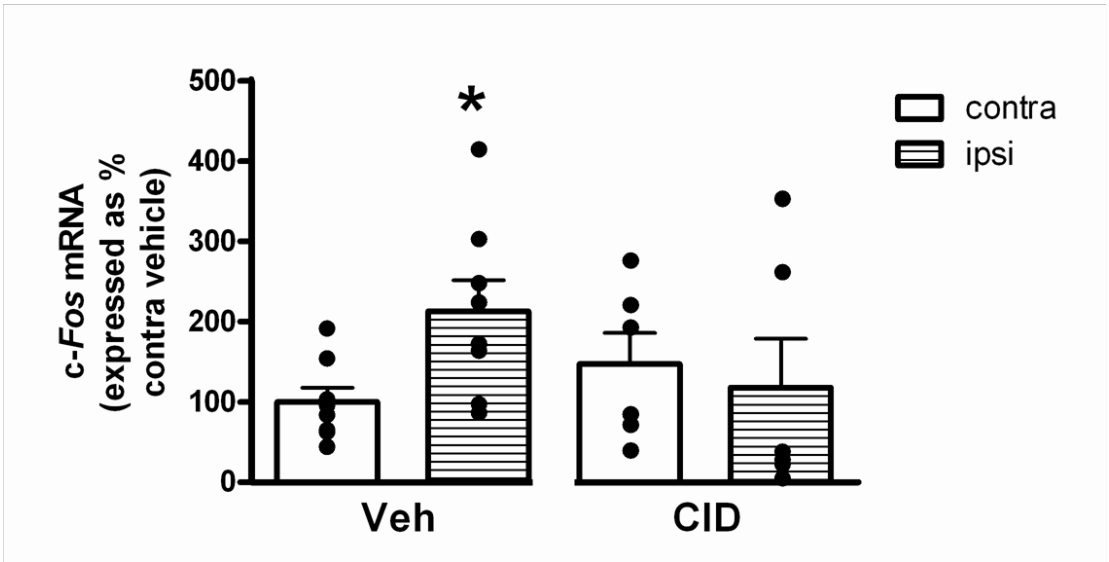

Figure 4 Effects of bilateral microinjections of CID16020046 into the ACC on levels of c-*Fos* mRNA in the spinal cord dorsal horn. Formalin treatment significantly increased levels of c-*Fos* mRNA in the ipsilateral spinal cord in vehicle-treated treated rats**.** Injection of CID16020046 into the ACC prevented the formalin-induced increase in c-*Fos* mRNA levels in the ipsilateral spinal cord dorsal horn**.** Data are mean ± SEM, *p<0.05, vs veh-contra, Student's unpaired t-test. Individual data points superimposed as black dots on bar graphs. Vehicle, n = 8 and CID16020046, n = 6 rats per group, contra; contralateral, ipsi; ipsilateral.

Intra-ACC administration of CID16020046 prevented formalin-induced increases in c-Fos mRNA levels in the ipsilateral spinal cord

In vehicle-treated rats, intraplantar administration of formalin resulted in a significant ($p<0.05$) increase in levels of c-*Fos* mRNA in the ipsilateral side of the spinal cord dorsal horn compared with the contralateral side. However, this formalin-induced increase in ipsilateral c-*Fos* expression was prevented in rats receiving intra-ACC administration of CID16020046 (Figure 4).

Endogenous levels of 2-Arachidonoyl-sn-glycerol-3-phosphoinositol are reduced in formalin-treated rats

The levels of 2-arachidonoyl-sn-glycerol-3-phosphoinositol (2-AGPI), a potent endogenous agonist of GPR55, were measured in the ACC of separate groups of rats, 30 mins after they had received intraplantar injections of formalin or saline into the right hind-paw. The 30-minute time point was chosen on the basis that it coincided with the maximum effects of CID16020046 in the pharmacological studies which also represented the peak phase of formalin-evoked nociceptive behaviour (Experiment 1). LC-MS/MS analysis revealed a significant ($p<0.05$) reduction in levels of 2-AGPI in the ACC of formalin-treated rats, compared with saline-treated counterparts (Figure 5A). Representative chromatograms and calibration curve for 2-AGPI are depicted in Figures 5B and 5C, respectively.

Fig 5

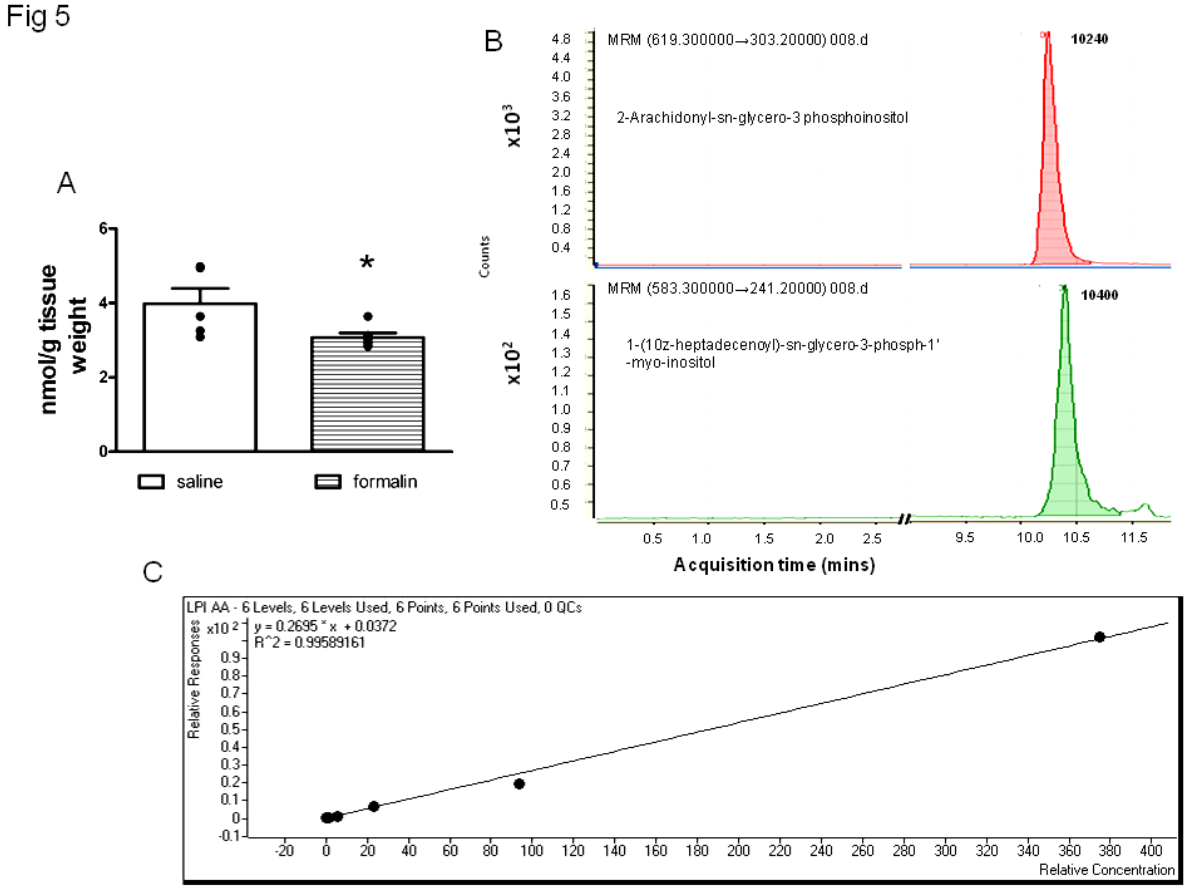

Figure 5. LC-MS/MS analysis of 2-arachidonoyl-sn-glycero-3-phosphoinositol (2-AGPI) in the rat ACC. (A) Comparison of 2-AGPI levels in the ACC of saline and formalin-treated rats, (**B**) Representative chromatograms and precursor and product ion mass-to-charge (m/z) ratio for 2-AGPI (619.30000- 303.20000; top panel) and 1-(10Z-heptadecenoyl)-sn-glycero-3-phospho-1'-myo-inositol) used as internal standard (583.30000-241.20000, bottom panel), (**C**) Calibration curve for 2-AGPI quantitation. Data are mean ± SEM **p*<0.05. Individual data points superimposed as black dots on bar graphs Student's unpaired t-test with Welch's correction. saline, n=5 and formalin n=6 rats per group.

Discussion

The present study investigated the role of GPR55 receptor signalling in the rat ACC in formalin-evoked nociceptive behaviour and the underlying molecular mechanisms. First, the expression of GPR55 in the ACC and in whole rat brain homogenates was confirmed by western blotting analysis which revealed immunoreactive bands at ~37kDa, consistent with the predicted molecular weight of GPR55 protein reported in literature (Pineiro et al., 2011). Further characterisation of GPR55 expression in the ACC using immunofluorescence histochemistry revealed a strong co-localisation between GPR55 and the neuronal marker, NeuN, but not the astrocyte or microglia markers, GFAP and IBA-1, respectively, in the ACC. These novel findings demonstrate a predominant expression of GPR55 on neurones rather than non-neuronal cells and suggest that, direct modulation of neuronal activity may underlie the effects of endogenous GPR55 signalling in the ACC. Intra-ACC administration of the selective GPR55 antagonist, CID16020046, significantly reduced the second phase of formalin-evoked nociceptive behaviour in rats. In addition, analysis of post-mortem ACC tissue revealed a robust reduction in ERK (1/2) protein phosphorylation in the ACC of rats that had received microinjection of CID16020046 into the ACC. Previously published work from our laboratory revealed significantly higher levels of pERK in the ACC of formalin-treated rats compared with saline-treated counterparts (Butler *et al.*, 2011). Furthermore, increased pERK induction in the ACC in response to formalin injection has also been demonstrated in other studies based on animal models of inflammatory pain (Wei *et al.*, 2008; Toyoda *et al.*, 2009). Collectively, these findings demonstrate an association between increased ERK phosphorylation and the development of pain states. Thus the suppression of ERK phosphorylation in the presence of nociceptive tone (i.e. formalin treatment) may be an important mechanism that underpins the antinociceptive effects of CID16020046. Furthermore, CID16020046 treatment prevented formalin-induced increases in c-*Fos* mRNA expression in ipsilateral spinal cord dorsal horn compared with the contralateral side. Importantly, locomotor activity, rearing and grooming

prior to formalin injection were not altered by CID16020046, suggesting that changes in these parameters were unlikely to be confounding factors in the effects of CID16020046 on formalin-evoked nociceptive behaviour. In summary, these data suggest a facilitatory or pronociceptive role for GPR55 signalling in the ACC in inflammatory pain, effects possibly mediated locally by ERK (1/2) phosphorylation and via top-down modulation of descending pain control.

The suggestion of a pronociceptive or facilitatory role for GPR55 activation in the ACC within the CNS is consistent with findings from a previous study demonstrating a similar role for GPR55 in the PAG (Deliu et al., 2015). In the study by Deliu and colleagues, direct intra-PAG microinjection of LPI, an endogenous ligand of GPR55 (Oka et al., 2007), was associated with reduced response latencies to noxious thermal stimuli in rats exposed to the hotplate test, an effect that was prevented by co-administration with a selective GPR55 antagonist, clearly demonstrating a role for GPR55 in mediating the pronociceptive effects of LPI. Moreover, Deliu and colleagues demonstrated an antinociceptive effect (to noxious thermal stimulation) following selective blockade of GPR55 in the PAG, a finding similar to our observation, reported herein, of reduced formalin-evoked nociceptive behaviour following the microinjection of the GPR55 antagonist CID16020046 into the ACC. Taken together, these findings reveal a facilitatory role for endogenously active GPR55 signalling in discrete brain regions associated with nociceptive processing within the CNS.

Activation of GPR55 in the ACC during inflammatory pain states is likely facilitated by the release and binding of endogenous GPR55 ligands including 2-AGPI, a potent endogenous ligand of GPR55 in the rat brain (Oka et al., 2009). Such release and subsequent degradation of 2-AGPI by endogenous lipases (Murase and Okuyama, 1985, Kobayashi et al, 1996) might be expected to result in a reduction in tissue levels of 2-AGPI in inflammatory pain states. Indeed, in the present study, we observed reduced tissue levels of 2-AGPI in the ACC of

formalin-treated rats compared with their saline-treated counterparts, likely reflecting increased release and subsequent degradation of 2-AGPI in the ACC following formalin injection. Moreover, the demonstration of a lysophosphatidyl inositol (LPI)-specific phoshospholipase lipase C (lysoPI-PLC) activity in synaptic plasma membranes of the rat brain (Kobayashi et al, 1996) provides a possible mechanism for the regulation of 2-AGPI-mediated GPR55 signalling. This interpretation is also consistent with the tight regulation of other endogenous lipid signalling molecules such as anandamide (AEA) and 2-arachidonoylglycerol (2-AG) by endogenous hydrolytic enzymes such as FAAH and MAGL, respectively. To the best of our knowledge, this finding represents the first evidence for involvement of an endogenous molecular species of LPI in the formalin model of tonic persistent inflammatory pain. The pronociceptive role of GPR55 signalling in the CNS and, in particular the ACC, may represent a functionally relevant physiological mechanism that enables the organism to perceive pain and take the necessary action to escape harm. Such a view is consistent with the role of the ACC as a key substrate for the modulation of affective and cognitive components of the pain experience (Fuchs et al., 2014)

The reduction in ERK (1/2) phosphorylation following the injection of the antagonist CID16020046 suggests that ERK (1/2) phosphorylation may be a direct or indirect downstream molecular mechanism mediating the effects of GPR55 signalling in the ACC on formalin-evoked nociceptive behaviour in rats. The roles of ERK (1/2) activation in the ACC in modulating pain-related negative affect (Cao et al., 2009, Dai et al., 2011, Zhong et al., 2012) and facilitation of thalamo-cortical ascending nociceptive transmission (Wei and Zhuo, 2008) have previously been demonstrated in animal models of inflammatory and neuropathic pain. These findings, when taken together, suggest that GPR55 signalling in the ACC, via ERK (1/2)

activation, may play a role in both the affective and sensory components of nociceptive processing within the CNS.

As described in the introductory paragraph of this manuscript, the descending pain pathway, of which the PAG is a key component, receives input from higher brain centres such as the ACC. This anatomical arrangement also raises the possibility of a top-down modulatory influence of GPR55 signalling in the ACC on the descending pain pathway. This view is further strengthened by the demonstration herein of suppressed formalin-induced increases in mRNA for c-*Fos*, a marker of neuronal activity (Hunt et al., 1987) in the spinal cord dorsal horn following injections of CID16020046 into the ACC. The nature of this modulatory influence of GPR55 signalling in the ACC on the descending pain pathway however remains unclear, given that the descending pain pathway may be inhibitory or facilitatory (Ossipov et al., 2014). In this regard, the effects of selective GPR55 blockade on the induction of c-*Fos* mRNA in the spinal cord dorsal horn may either reflect an enhancement of the inhibitory descending pain pathway or suppression of the facilitatory component. Conversely the endogenous activation of GPR55 in the ACC is likely to modulate the descending pain pathway in a manner that will increase or enhance central sensitization of spinal cord dorsal neurons. Thus, given that the antinociceptive effects of CID16020046 in the present study were mainly restricted to the second phase of formalin-evoked nociceptive behaviour, a significant component of which is driven by central sensitization mechanisms (Coderre et al., 1990, Hunskaar and Hole, 1987, Shimoyama et al., 1997), it seems plausible that descending pain facilitation may constitute an important mechanism by which endogenously activated GPR55 in the ACC modulates neuronal activity within the spinal cord.

In conclusion, these data demonstrate that endogenous activation of GPR55 in the rat ACC may contribute to the development of a persistent inflammatory pain state and provide further support for GPR55 signalling as a therapeutic target for the treatment of inflammatory pain.

Acknowledgements: This work was funded by a research grant from Science Foundation Ireland (10/IN.1/B2976) and from Conselho Nacionalde Desenvolvimento Cientifico e Tecnologico, Brazil (CNPq; 207530/2014-9).

Disclosures: The authors have no conflicts of interest to declare.

References

AN, X., BANDLER, R., ONGUR, D. & PRICE, J. L. (1998) Prefrontal cortical projections to longitudinal columns in the midbrain periaqueductal gray in macaque monkeys. *J Comp Neurol,* 401**,** 455-79.

BARTHAS, F., SELLMEIJER, J., HUGEL, S., WALTISPERGER, E., BARROT, M. & YALCIN, I. (2015) The Anterior Cingulate Cortex Is a Critical Hub for Pain-Induced Depression. *Biological Psychiatry,* 77**,** 236-245.

BASBAUM, A. I. & FIELDS, H. L. (1984) Endogenous pain control systems: brainstem spinal pathways and endorphin circuitry. *Annu Rev Neurosci,* 7**,** 309-38.

BRADFORD, M. M. (1976) A rapid and sensitive method for the quantitation of microgram quantities of protein utilizing the principle of protein-dye binding. *Anal Biochem,* 72**,** 248-54.

BREEN, C., BROWNJOHN, P. W. & ASHTON, J. C. (2012) The atypical cannabinoid O-1602 increases hind paw sensitisation in the chronic constriction injury model of neuropathic pain. *Neurosci Lett,* 508**,** 119-22.

BUTLER, R. K., NILSSON-TODD, L., CLEREN, C., LÉNA, I., GARCIA, R. & FINN, D. P. (2011) Molecular and electrophysiological changes in the prefrontal cortex–amygdala–dorsal periaqueductal grey pathway during persistent pain state and fear-conditioned analgesia. *Physiology & Behavior,* 104**,** 1075-1081.

CAO, H., GAO, Y.-J., REN, W.-H., LI, T.-T., DUAN, K.-Z., CUI, Y.-H., CAO, X.-H., ZHAO, Z.-Q., JI, R.-R. & ZHANG, Y.-Q. (2009) Activation of Extracellular Signal-Regulated Kinase in the Anterior Cingulate Cortex Contributes to the Induction and Expression of Affective Pain. *The Journal of Neuroscience,* 29**,** 3307-3321.

CAREY, L. M., GUTIERREZ, T., DENG, L., LEE, W.-H., MACKIE, K. & HOHMANN, A. G. (2017) Inflammatory and Neuropathic Nociception is Preserved in GPR55 Knockout Mice. *Scientific Reports,* 7**,** 944.

CODERRE, T. J., VACCARINO, A. L. & MELZACK, R. (1990) Central nervous system plasticity in the tonic pain response to subcutaneous formalin injection. *Brain Res,* 535**,** 155-8.

CONNELL, K., BOLTON, N., OLSEN, D., PIOMELLI, D. & HOHMANN, A. G. (2006) Role of the basolateral nucleus of the amygdala in endocannabinoid-mediated stress-induced analgesia. *Neurosci Lett,* 397**,** 180-4.

DAI, M. D. P. D. R.-P., LI, P. D. C.-Q., ZHANG, P. D. J.-W., LI, P. D. F., SHI, B. M. X.-D., ZHANG, P. D. J.-Y. & ZHOU, P. D. X.-F. (2011) Biphasic Activation of Extracellular Signal-regulated Kinase in Anterior Cingulate Cortex Distinctly Regulates the

Development of Pain-related Anxiety and Mechanical Hypersensitivity in Rats after Incision. *Anesthesiology,* 115**,** 604-613.

DELIU, E., SPEROW, M., CONSOLE-BRAM, L., CARTER, R. L., TILLEY, D. G., KALAMARIDES, D. J., KIRBY, L. G., BRAILOIU, G. C., BRAILOIU, E., BENAMAR, K. & ABOOD, M. E. (2015) The Lysophosphatidylinositol Receptor GPR55 Modulates Pain Perception in the Periaqueduactal Grey. *Molecular Pharmacology*.

DONAHUE, R. R., LAGRAIZE, S. C. & FUCHS, P. N. (2001) Electrolytic lesion of the anterior cingulate cortex decreases inflammatory, but not neuropathic nociceptive behavior in rats. *Brain Research,* 897**,** 131-138.

FINN, D. P., CHAPMAN, V., JHAVERI, M. D., SAMANTA, S., MANDERS, T., BOWDEN, J., MATTHEWS, L., MARSDEN, C. A. & BECKETT, S. R. (2003) The role of the central nucleus of the amygdala in nociception and aversion. *Neuroreport,* 14**,** 981-4.

FUCHS, P. N., PENG, Y. B., BOYETTE-DAVIS, J. A. & UHELSKI, M. L. (2014) The anterior cingulate cortex and pain processing. *Front Integr Neurosci,* 8**,** 35.

GANGADHARAN, V., SELVARAJ, D., KUREJOVA, M., NJOO, C., GRITSCH, S., SKORICOVA, D., HORSTMANN, H., OFFERMANNS, S., BROWN, A. J., KUNER, T., TAPPE-THEODOR, A. & KUNER, R. (2013) A novel biological role for the phospholipid lysophosphatidylinositol in nociceptive sensitization via activation of diverse G-protein signalling pathways in sensory nerves in vivo. *PAIN,* 154**,** 2801-12.

GUY, A. T., NAGATSUKA, Y., OOASHI, N., INOUE, M., NAKATA, A., GREIMEL, P., INOUE, A., NABETANI, T., MURAYAMA, A., OHTA, K., ITO, Y., AOKI, J., HIRABAYASHI, Y. & KAMIGUCHI, H. (2015) Glycerophospholipid regulation of modality-specific sensory axon guidance in the spinal cord. *Science,* 349**,** 974.

HENSTRIDGE, C. M., BALENGA, N. A., KARGL, J., ANDRADAS, C., BROWN, A. J., IRVING, A., SANCHEZ, C. & WALDHOER, M. (2011) Minireview: recent developments in the physiology and pathology of the lysophosphatidylinositol-sensitive receptor GPR55. *Mol Endocrinol,* 25**,** 1835-48.

HEYNEN-GENEL S, D. R., SHI S, ET AL. (2010) Screening for Selective Ligands for GPR55 - Antagonists. *[Updated 2011 May 26]. In: Probe Reports from the NIH Molecular Libraries Program [Internet]. Bethesda (MD): National Center for Biotechnology Information.*

HOHMANN, A. G., SUPLITA, R. L., BOLTON, N. M., NEELY, M. H., FEGLEY, D., MANGIERI, R., KREY, J. F., WALKER, J. M., HOLMES, P. V., CRYSTAL, J. D., DURANTI, A., TONTINI, A., MOR, M., TARZIA, G. & PIOMELLI, D. (2005) An endocannabinoid mechanism for stress-induced analgesia. *Nature,* 435**,** 1108-12.

HUNSKAAR, S. & HOLE, K. (1987) The formalin test in mice: dissociation between inflammatory and non-inflammatory pain. *PAIN,* 30**,** 103-14.

HUNT, S. P., PINI, A. & EVAN, G. (1987) Induction of c-fos-like protein in spinal cord neurons following sensory stimulation. *Nature,* 328**,** 632-4.

JOHANSEN, J., FIELDS, H. & MANNING, B. (2001) The affective component of pain in rodents: direct evidence for a contribution of the anterior cingulate cortex. *Proc Natl Acad Sci USA,* 98**,** 8077 - 82.

KARGL, J., BROWN, A. J., ANDERSEN, L., DORN, G., SCHICHO, R., WALDHOER, M. & HEINEMANN, A. (2013) A selective antagonist reveals a potential role of G protein-coupled receptor 55 in platelet and endothelial cell function. *J Pharmacol Exp Ther,* 346**,** 54-66.

KILKENNY, C., BROWNE, W., CUTHILL, I. C., EMERSON, M. & ALTMAN, D. G. (2010) Animal research: reporting in vivo experiments: the ARRIVE guidelines. *Br J Pharmacol,* 160**,** 1577-9.

KOBAYASHI,T; KISHIMOTO M, OKUYAMA, H (1996) Phospholipases involved in lysophosphatidylinositol metabolism in rat brain J. Lipid Mediators Cell Signalling 14, 33-37

MASQUELIER, J. & MUCCIOLI, G. G. (2016) Development and validation of a specific and sensitive HPLC-ESI-MS method for quantification of lysophosphatidylinositols and evaluation of their levels in mice tissues. *J Pharm Biomed Anal,* 126**,** 132-40.

MURASE, S. & OKUYAMA, H. (1985) A membrane-bound phospholipase C with an apparent specificity for lysophosphatidylinositol in porcine platelets. *J Biol Chem,* 260**,** 262-5.

OKA, S., NAKAJIMA, K., YAMASHITA, A., KISHIMOTO, S. & SUGIURA, T. (2007) Identification of GPR55 as a lysophosphatidylinositol receptor. *Biochem Biophys Res Commun,* 362**,** 928-34.

OKA, S., TOSHIDA, T., MARUYAMA, K., NAKAJIMA, K., YAMASHITA, A. & SUGIURA, T. (2009) 2-Arachidonoyl-sn-glycero-3-phosphoinositol: a possible natural ligand for GPR55. *J Biochem,* 145**,** 13-20.

OKINE, B., NORRIS, L., WOODHAMS, S., BURSTON, J., PATEL, A., ALEXANDER, S., BARRETT, D., KENDALL, D., BENNETT, A. & CHAPMAN, V. (2012a) Lack of effect of chronic pre-treatment with the FAAH inhibitor URB597 on inflammatory pain behaviour: evidence for plastic changes in the endocannabinoid system. *British Journal of Pharmacology,* 167**,** 627-640.

OKINE, B. N., NORRIS, L. M., WOODHAMS, S., BURSTON, J., PATEL, A., ALEXANDER, S. P., BARRETT, D. A., KENDALL, D. A., BENNETT, A. J. &

CHAPMAN, V. (2012b) Lack of effect of chronic pre-treatment with the FAAH inhibitor URB597 on inflammatory pain behaviour: evidence for plastic changes in the endocannabinoid system. *Br J Pharmacol,* 167**,** 627-40.

OKINE, B. N., REA, K., OLANGO, W. M., PRICE, J., HERDMAN, S., MADASU, M. K., ROCHE, M. & FINN, D. P. (2014) A role for PPARalpha in the medial prefrontal cortex in formalin-evoked nociceptive responding in rats. *Br J Pharmacol,* 171**,** 1462-71.

OLANGO, W. M., ROCHE, M., FORD, G. K., HARHEN, B. & FINN, D. P. (2011) The endocannabinoid system in the rat dorsolateral periaqueductal grey mediates fear-conditioned analgesia and controls fear expression in the presence of nociceptive tone. *Br J Pharmacol,* 165**,** 2549-60.

OSSIPOV, M. H., DUSSOR, G. O. & PORRECA, F. (2010) Central modulation of pain. *The Journal of Clinical Investigation,* 120**,** 3779-3787.

OSSIPOV, M. H., MORIMURA, K. & PORRECA, F. (2014) Descending pain modulation and chronification of pain. *Current Opinion in Supportive and Palliative Care,* 8**,** 143-151.

PAXINOS, G. & WATSON, C. (1986) The Rat Brain in Stereotaxic Coordinates.

PINEIRO, R., MAFFUCCI, T. & FALASCA, M. (2011) The putative cannabinoid receptor GPR55 defines a novel autocrine loop in cancer cell proliferation. *Oncogene,* 30**,** 142-152.

QU, C., KING, T., OKUN, A., LAI, J., FIELDS, H. L. & PORRECA, F. (2011) Lesion of the Rostral Anterior Cingulate Cortex Eliminates the Aversiveness of Spontaneous Neuropathic Pain Following Partial or Complete Axotomy. *PAIN,* 152**,** 1641-1648.

RAINVILLE, P., DUNCAN, G. H., PRICE, D. D., CARRIER, B. T. & BUSHNELL, M. C. (1997) Pain Affect Encoded in Human Anterior Cingulate But Not Somatosensory Cortex. *Science,* 277**,** 968.

REA, K., OLANGO, W. M., OKINE, B. N., MADASU, M. K., MCGUIRE, I. C., COYLE, K., HARHEN, B., ROCHE, M. & FINN, D. P. (2014) Impaired endocannabinoid signalling in the rostral ventromedial medulla underpins genotype-dependent hyper-responsivity to noxious stimuli. *PAIN,* 155**,** 69-79.

ROCHE, M., O'CONNOR, E., DISKIN, C. & FINN, D. P. (2007) The effect of CB(1) receptor antagonism in the right basolateral amygdala on conditioned fear and associated analgesia in rats. *Eur J Neurosci,* 26**,** 2643-53.

ROCHE, M., JOHNSTON, P., MHUIRCHEARTAIGH, O. N., OLANGO, W. M., MACKIE, K. & FINN, D. P. (2010) Effects of intra-basolateral amygdala administration of rimonabant on nociceptive behaviour and neuronal activity in the presence or absence of contextual fear. *Eur J Pain,* 14**,** 487-95.

ROSS, R. A. (2009) The enigmatic pharmacology of GPR55. *Trends Pharmacol Sci,* 30**,** 156-163.

SCHUELERT, N. & MCDOUGALL, J. J. (2011) The abnormal cannabidiol analogue O-1602 reduces nociception in a rat model of acute arthritis via the putative cannabinoid receptor GPR55. *Neurosci Lett,* 500**,** 72-6.

SHACKMAN, A. J., SALOMONS, T. V., SLAGTER, H. A., FOX, A. S., WINTER, J. J. & DAVIDSON, R. J. (2011) The integration of negative affect, pain and cognitive control in the cingulate cortex. *Nat Rev Neurosci,* 12**,** 154-67.

SHARIR, H. & ABOOD, M. E. (2010) Pharmacological characterization of GPR55, a putative cannabinoid receptor. *Pharmacol Ther,* 126**,** 301-13.

SHIMOYAMA, N., SHIMOYAMA, M., DAVIS, A. M., INTURRISI, C. E. & ELLIOTT, K. J. (1997) Spinal gabapentin is antinociceptive in the rat formalin test. *Neuroscience Letters,* 222**,** 65-67.

STATON, P. C., HATCHER, J. P., WALKER, D. J., MORRISON, A. D., SHAPLAND, E. M., HUGHES, J. P., CHONG, E., MANDER, P. K., GREEN, P. J., BILLINTON, A., FULLEYLOVE, M., LANCASTER, H. C., SMITH, J. C., BAILEY, L. T., WISE, A., BROWN, A. J., RICHARDSON, J. C. & CHESSELL, I. P. (2008) The putative cannabinoid receptor GPR55 plays a role in mechanical hyperalgesia associated with inflammatory and neuropathic pain. *PAIN,* 139**,** 225-36.

SUPLITA, R. L., 2ND, FARTHING, J. N., GUTIERREZ, T. & HOHMANN, A. G. (2005) Inhibition of fatty-acid amide hydrolase enhances cannabinoid stress-induced analgesia: sites of action in the dorsolateral periaqueductal gray and rostral ventromedial medulla. *Neuropharmacology,* 49**,** 1201-9.

TOYODA, H., ZHAO, M.-G., ULZHÖFER, B., WU, L.-J., XU, H., SEEBURG, P. H., SPRENGEL, R., KUNER, R. & ZHUO, M. (2009) Roles of the AMPA receptor subunit GluA1 but not GluA2 in synaptic potentiation and activation of ERK in the anterior cingulate cortex. *Molecular Pain,* 5**,** 46-46.

VALET, M., SPRENGER, T., BOECKER, H., WILLOCH, F., RUMMENY, E., CONRAD, B., ERHARD, P. & TOLLE, T. R. (2004) Distraction modulates connectivity of the

cingulo-frontal cortex and the midbrain during pain—an fMRI analysis. *PAIN,* 109**,** 399-408.

VIUDEZ-MARTÍNEZ, A., GARCÍA-GUTIÉRREZ, M. S., NAVARRÓN, C. M., MORALES-CALERO, M. I., NAVARRETE, F., TORRES-SUÁREZ, A. I. & MANZANARES, J. (2017) Cannabidiol reduces ethanol consumption, motivation and relapse in mice. *Addiction Biology***,** n/a-n/a.

WATSON, G. S., SUFKA, K. J. & CODERRE, T. J. 1997. Optimal scoring strategies and weights for the formalin test in rats. *Pain,* 70**,** 53-58.

WEI, F. & ZHUO, M. (2008) Activation of Erk in the anterior cingulate cortex during the induction and expression of chronic pain. *Mol Pain,* 4**,** 28.

ZHONG, X.-L., WEI, R., ZHOU, P., LUO, Y.-W., WANG, X.-Q., DUAN, J., BI, F.-F., ZHANG, J.-Y., LI, C.-Q., DAI, R.-P. & LI, F. (2012) Activation of Anterior Cingulate Cortex Extracellular Signal-Regulated Kinase-1 and -2 (ERK1/2) Regulates Acetic Acid-Induced, Pain-Related Anxiety in Adult Female Mice. *Acta Histochemica et Cytochemica,* 45**,** 219-225.

Fig 1

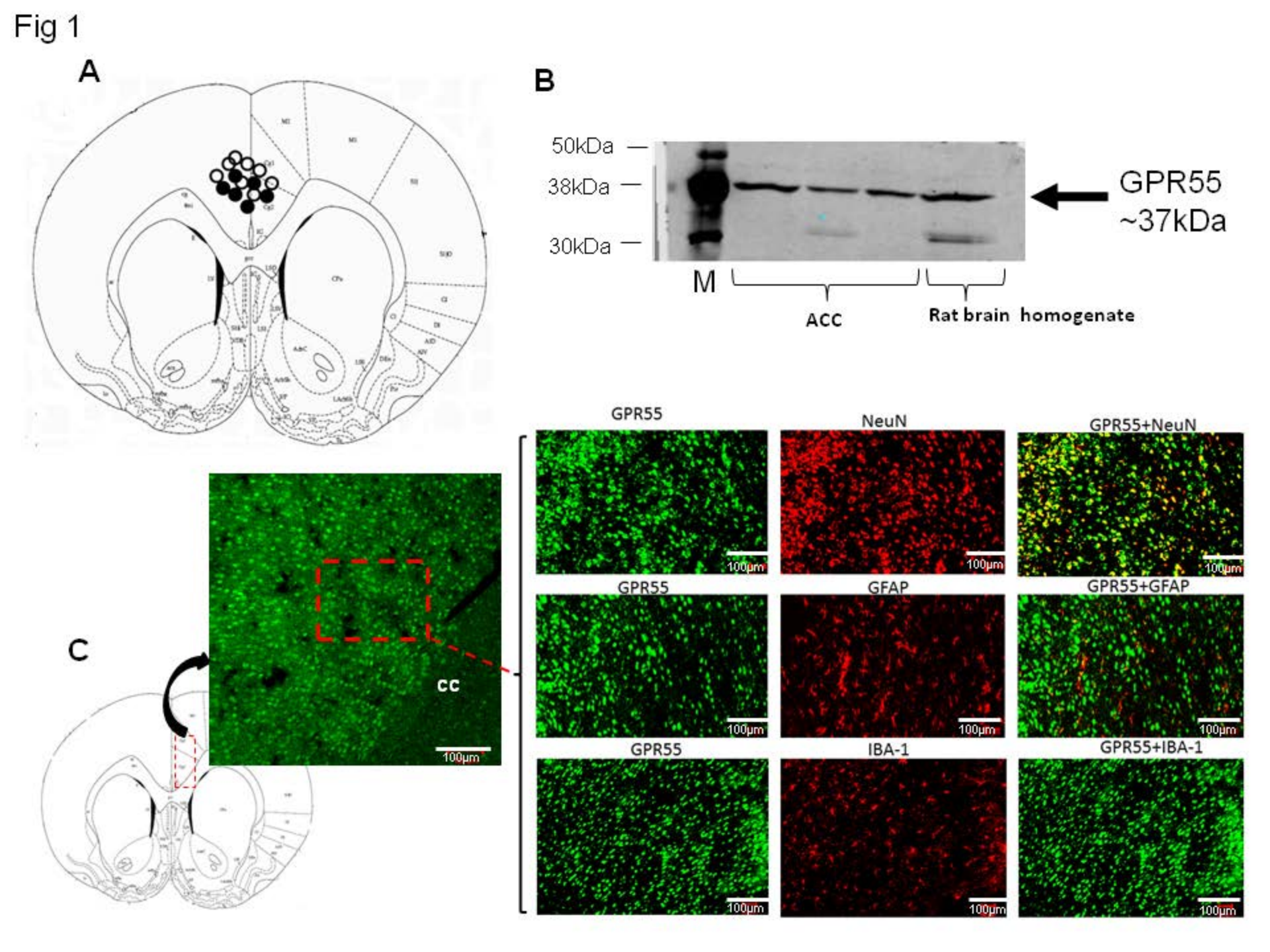
A
B
50kDa
38kDa
30kDa
GPR55
~37kDa
M
ACC
Rat brain homogenate
C
cc
100μm
GPR55
NeuN
GPR55+NeuN
GFAP
GPR55+GFAP
IBA-1
GPR55+IBA-1

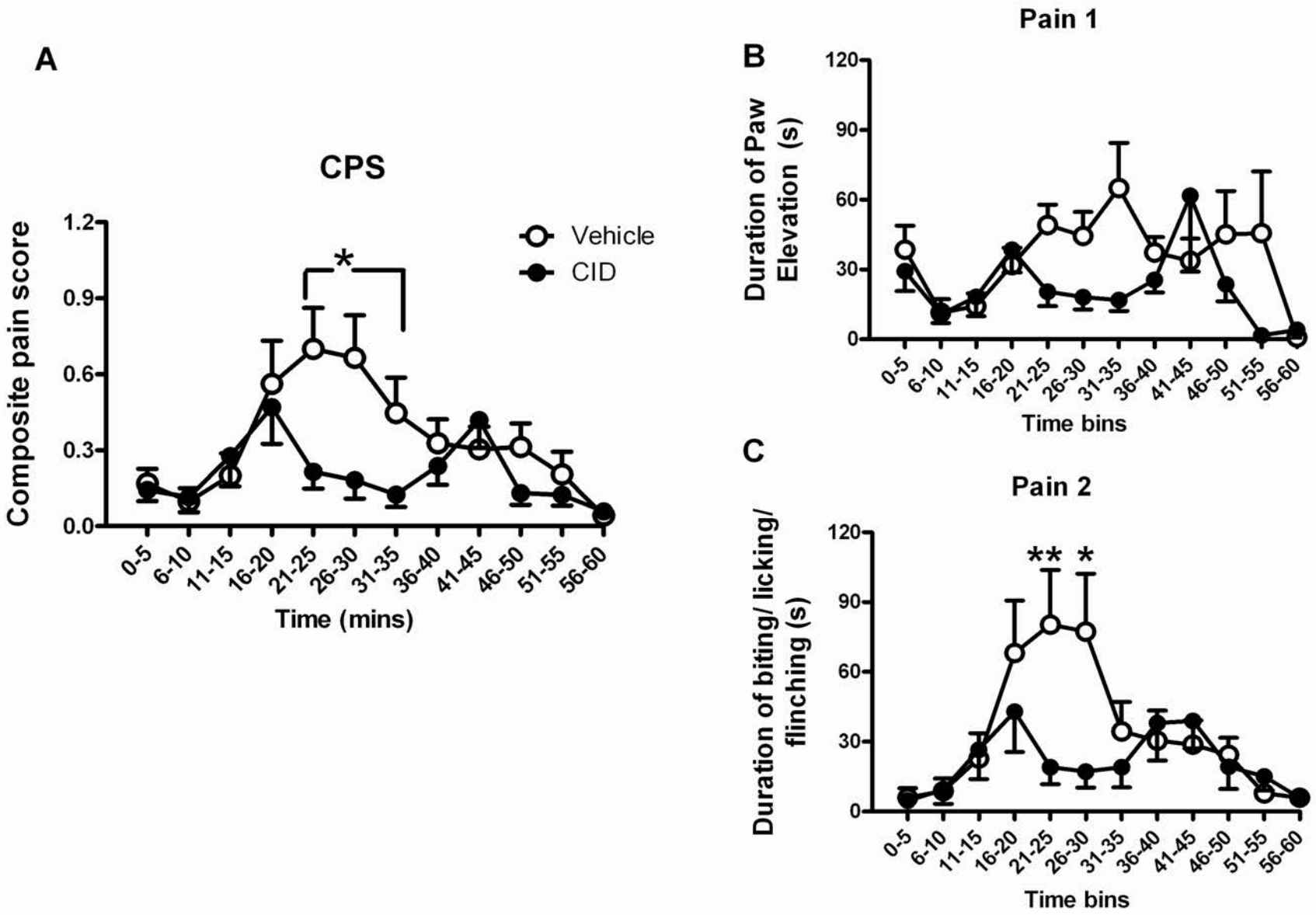
A
CPS
Composite pain score
1.2
0.9
0.6
0.3
0.0
Vehicle
CID
*
0-5
6-10
11-15
16-20
21-25
26-30
31-35
36-40
41-45
46-50
51-55
56-60
Time (mins)
B
Pain 1
Duration of Paw Elevation (s)
120
90
60
30
0
Time bins
C
Pain 2
Duration of biting/ licking/ flinching (s)
** *
Time bins

Fig 3

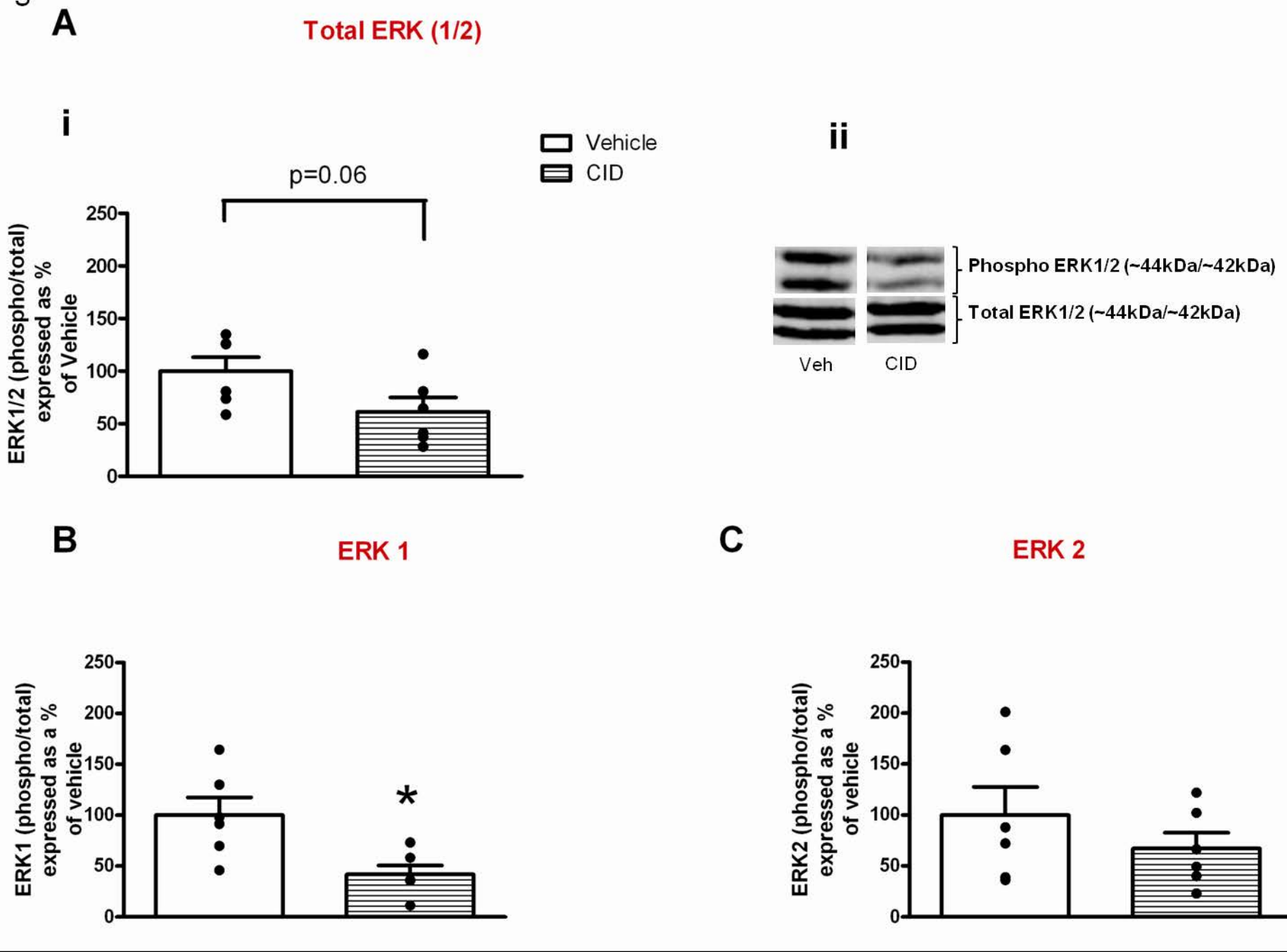
A
Total ERK (1/2)
i
Vehicle
CID
p=0.06
ERK1/2 (phospho/total) expressed as % of Vehicle
250
200
150
100
50
0
ii
Phospho ERK1/2 (~44kDa/~42kDa)
Total ERK1/2 (~44kDa/~42kDa)
Veh
CID
B
ERK 1
ERK1 (phospho/total) expressed as a % of vehicle
*
C
ERK 2
ERK2 (phospho/total) expressed as a % of vehicle

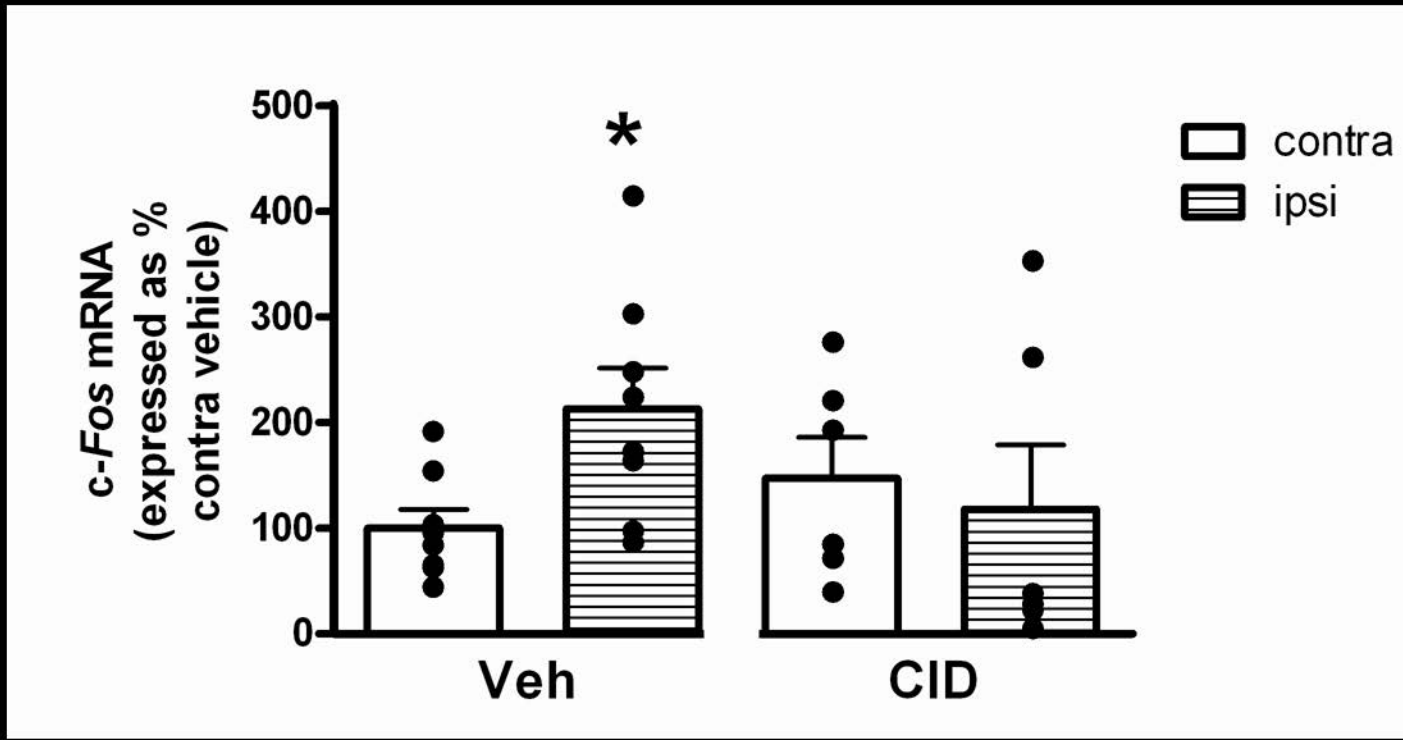
c-Fos mRNA
(expressed as %
contra vehicle)
500
400
300
200
100
0
*
Veh
CID
contra
ipsi

Fig 5

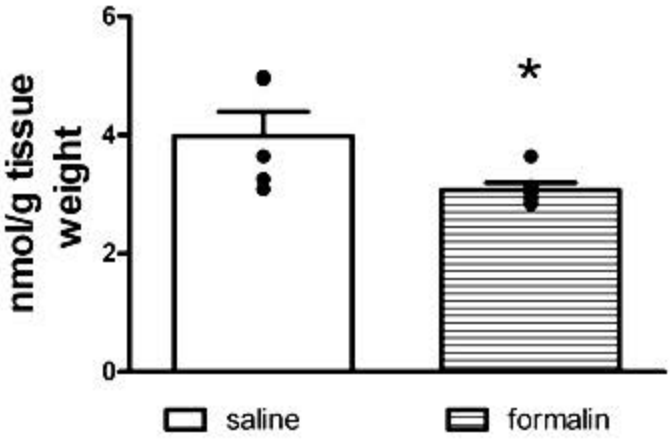
A
nmol/g tissue weight
6
4
2
0
*
saline
formalin

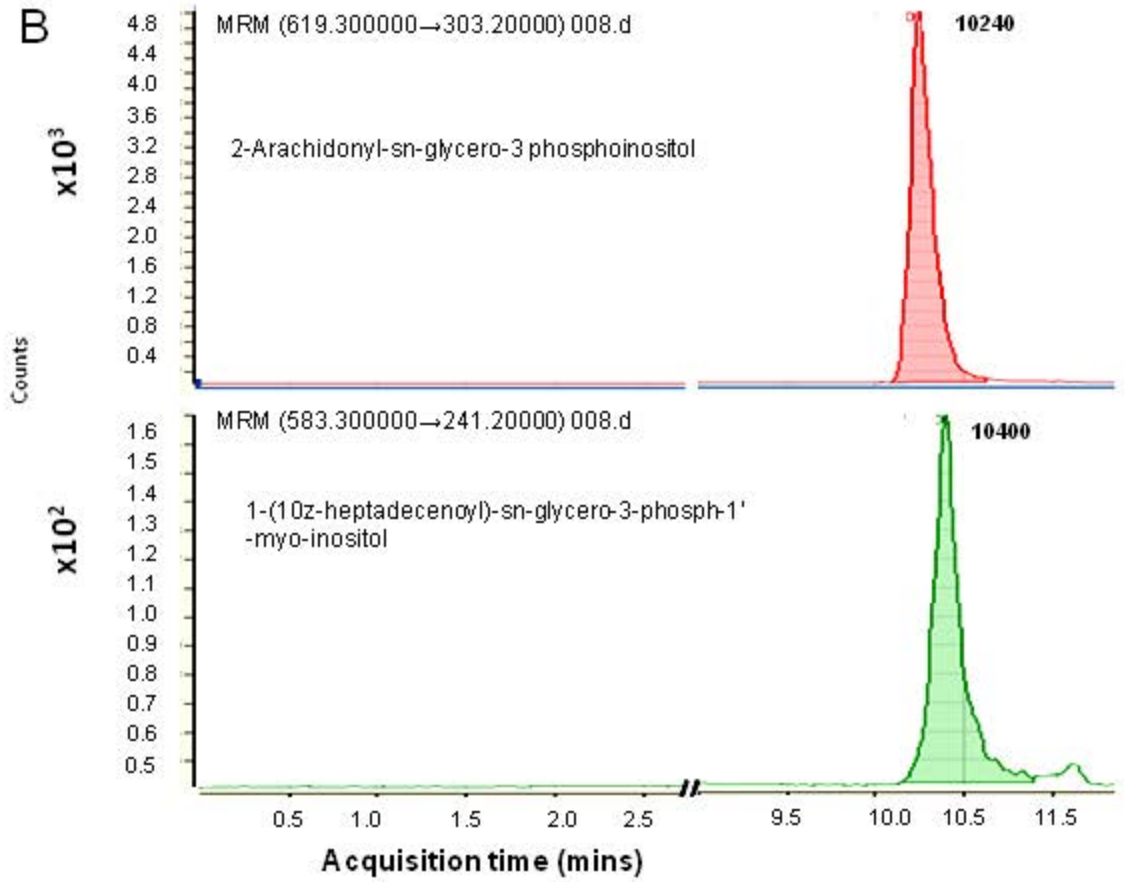
B
MRM (619.300000→303.20000) 008.d
10240
2-Arachidonyl-sn-glycero-3 phosphoinositol
x10³
4.8
4.4
4.0
3.6
3.2
2.8
2.4
2.0
1.6
1.2
0.8
0.4
Counts
MRM (583.300000→241.20000) 008.d
10400
1-(10z-heptadecenoyl)-sn-glycero-3-phosph-1'
-myo-inositol
x10²
1.6
1.5
1.4
1.3
1.2
1.1
1.0
0.9
0.8
0.7
0.6
0.5
0.5
1.0
1.5
2.0
2.5
9.5
10.0
10.5
11.5
Acquisition time (mins)

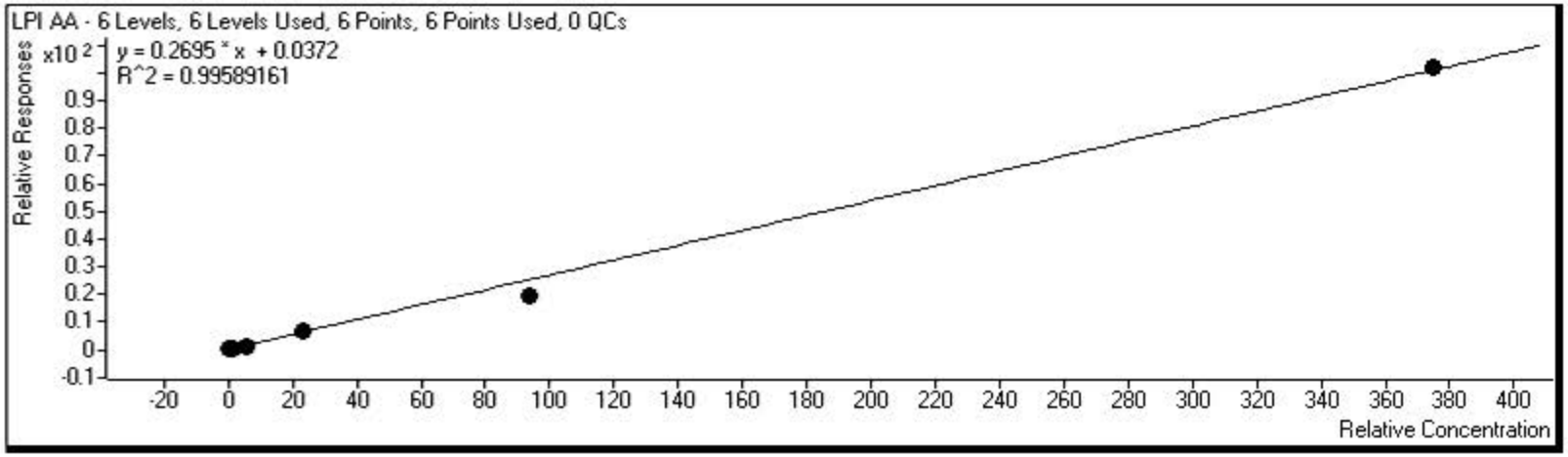
C
LPI AA - 6 Levels, 6 Levels Used, 6 Points, 6 Points Used, 0 QCs
y = 0.2695 * x + 0.0372
R^2 = 0.99589161
x10 2
Relative Responses
0.9
0.8
0.7
0.6
0.5
0.4
0.3
0.2
0.1
0
-0.1
-20
0
20
40
60
80
100
120
140
160
180
200
220
240
260
280
300
320
340
360
380
400
Relative Concentration